JACS
JOURNAL OF THE AMERICAN CHEMICAL SOCIETY
Communication
pubs.acs.org/JACS

Control of Molecular Rotor Rotational Frequencies in Porous Coordination Polymers Using a Solid-Solution Approach

Munehiro Inukai,[†] Tomohiro Fukushima,[‡] Yuh Hijikata,[§] Naoki Ogiwara,[‡] Satoshi Horike,*[,‡] and Susumu Kitagawa*[,†,‡]

[†]Institute for Integrated Cell-Material Sciences (iCeMS), Kyoto University, Yoshida, Sakyo-ku, Kyoto 606-8501, Japan

[‡]Department of Synthetic Chemistry and Biological Chemistry, Graduate School of Engineering, Kyoto University, Katsura, Nishikyo-ku, Kyoto 615-8510, Japan

[§]Institute of Transformative Bio-Molecules (WPI-ITbM), Nagoya University, Chikusa-ku, Nagoya 464-8602, Japan

Supporting Information

ABSTRACT: Rational design to control the dynamics of molecular rotors in crystalline solids is of interest because it offers advanced materials with precisely tuned functionality. Herein, we describe the control of the rotational frequency of rotors in flexible porous coordination polymers (PCPs) using a solid-solution approach. Solid-solutions of the flexible PCPs $[\{Zn(5\text{-nitroisophthalate})_x(5\text{-methoxyisophthalate})_{1-x}(\text{deuterated 4,4′-bipyridyl})\}(DMF{\cdot}MeOH)]_n$ allow continuous modulation of cell volume by changing the solid-solution ratio x. Variation of the isostructures provides continuous changes in the local environment around the molecular rotors (pyridyl rings of the 4,4′-bipyridyl group), leading to the control of the rotational frequency without the need to vary the temperature.

Material design to control molecular dynamics has been quite attractive for the development of molecular machines and devices.[1] Control of the dynamics of molecular rotors in crystalline solids is a particularly interesting challenge in chemistry and materials science because such control would enable the precise tuning and control of the functionality of these materials.[2] Aligned rotors in crystals collectively respond to external stimuli and afford dielectric,[3] magnetic,[4] and optical properties.[5] The rotational frequency (or rotational speed) directly affects the response behavior and the functionality. To date, a few studies have demonstrated change of the rotor rotational frequency in crystals by modifying the substituent groups around the rotors.[6] Systematic modification of the substituent groups changes the local environment and rotational frequency of the rotors; however, this strategy has not provided control (or continuous change) of the frequency due to the limited range of available substituent derivatives.

Porous coordination polymers (PCPs) and metal−organic frameworks (MOFs)[7] constructed of metal ions and organic ligands have great potential as crystalline solids that can allow the control of molecular rotor dynamics due to their porosity, thermal stability, and structural flexibility.[8] Specifically, the porosity of PCPs and MOFs provides sufficient space for the rotation of organic ligands. The shape and volume of the pores affects the rotational frequency of the ligands. In fact, rotative pillar ligands in PCPs and MOFs are regarded as highly ordered molecular rotors[8] and the rotations provide functions such as ferroelectricity, spin-crossover, and luminescence.[9]

In the present study, a solid-solution approach was adopted in order to modulate the rotational frequency of molecular rotors in PCPs. Binary solid-solutions in which two components are homogeneously mixed result in products with continuously changing crystal lattice parameters depending on the concentrations of the components (Vegard's law).[10] Recently, solid-solutions of PCPs with two or more types of ligands have been reported.[11] Herein we demonstrate the control of the rotational frequency of pillar ligand rotors in PCPs through the modulation of the void space using this solid-solution approach.

Solid-solutions of PCPs with an interdigitated structure (referred to as CIDs) were employed in the present study.[11c] Figure 1 shows the crystal structures of CID-5⊃G and CID-6⊃G $[\{Zn(5\text{-}NO_2\text{-ip})\ (bpy\text{-}d^8)\}(0.5DMF{\cdot}0.5MeOH)]_n$ (CID-5⊃G; 5-NO_2-ip = 5-nitroisophthalate, and bpy-d^8 = deuterated 4,4′-bipyridyl), and $[\{Zn(5\text{-MeO-ip})\ (bpy\text{-}d^8)\}(0.5\ DMF{\cdot}0.5\ MeOH)]_n$ (CID-6⊃G; 5-MeO-ip = 5-methoxyisophthalate)], where G denotes guest molecule (DMF and MeOH). In these materials, the bpy ligand was deuterated (bpy-d^8) to monitor the flip rotation via solid-state ^2H NMR. The pyridyl ring rotors in bpy were expected to rotate about the N−C axis.[12] According to the classification of (1) empty volume, (2) volume-conserving motions, and (3) correlated motions for the controllable molecular dynamics in crystalline solids,[6b] the compounds herein are categorized as empty volume. Thus, the rotation of the pyridyl ring rotors in CID-5⊃G and CID-6⊃G were first elucidated. CID-5⊃G is constructed from two-dimensional (2D) sheets composed of Zn^{2+}, 5-NO_2-ip, and the pillar ligand. The crystal structure has one-dimensional (1D) channels along the c axis in which MeOH and DMF are accommodated. One of the pyridyl rings in bpy is disordered with a dihedral angle of 24.9°. The crystal structure of CID-6⊃G is an isostructure of CID-5⊃G where 5-MeO-ip is used in place of 5-NO_2-ip. In both frameworks, the 2D sheets have a motif of interdigitation via $\pi-\pi$ stacking interactions between the benzene rings of 5-NO_2-ip or 5-MeO-ip. The difference between the NO_2 and MeO group affects the packing structure and void space, which is

Received: May 25, 2015
Published: September 14, 2015

DOI: 10.1021/jacs.5b05413
J. Am. Chem. Soc. 2015, 137, 12183−12186

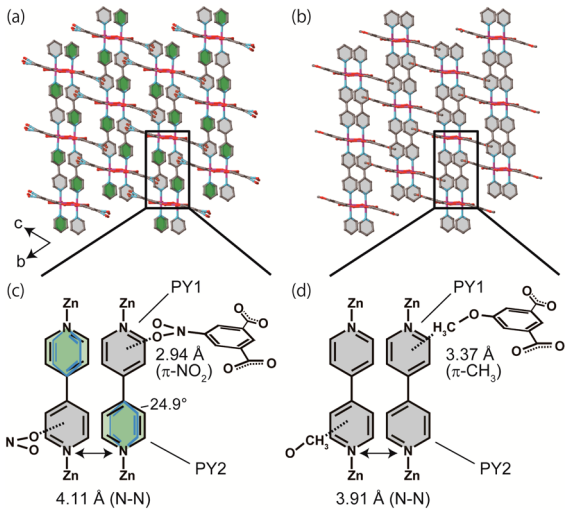

Figure 1. Packing structures of (a) $[\{Zn(5\text{-}NO_2\text{-ip})\ (bpy\text{-}d^8)\}\text{-}(0.5DMF{\cdot}0.5MeOH)]_n$ (CID-5⊃G) and (b) $[\{Zn(5\text{-}MeO\text{-ip})\ (bpy\text{-}d^8)\}(0.5\ DMF{\cdot}0.5\ MeOH)]_n$ (CID-6⊃G) at 293 K. Hydrogen and deuterium atoms are omitted for clarity. Schematic illustrations of the local environments of the pyridyl ring rotors in (c) CID-5⊃G and (d) CID-6⊃G. Green and gray in the pyridyl ring rotors represent the rotating and static moieties, respectively.

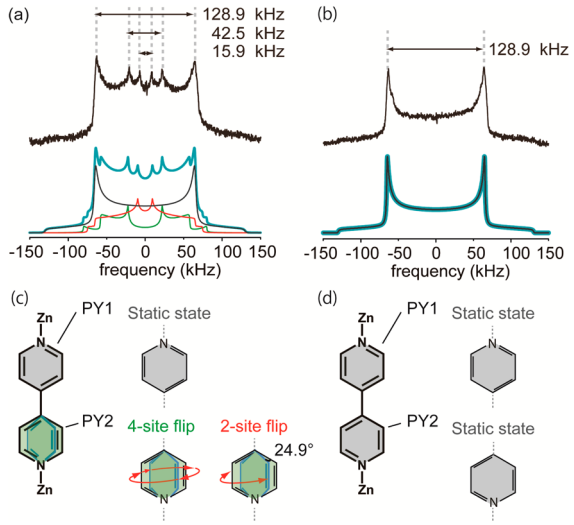

Figure 2. ^2H solid-state NMR spectra of (a) CID-5⊃G and (b) CID-6⊃G at 298 K. Black and blue lines indicate experimental and simulated spectra, respectively. The simulated spectra (blue) are composed of spectra reflecting a static state (gray), a 4-site flip of the pyridyl rings between 0, 24.9, 180, and 204.9° (green), and a 2-site flip between 24.9 and 180° (red). Illustrations of flip motions for PY1 and PY2 in (c) CID-5⊃G and (d) CID-6⊃G. Green and gray in the pyridyl ring rotors represent the rotational and static moieties, respectively.

expected to influence the rotational mode and frequency of the pyridyl ring rotors.

The local environment of the pyridyl ring rotors in bpy strongly affects the flip modes and frequencies of the rotors. The crystal structures of CID-5⊃G and CID-6⊃G revealed the existence of two types of pyridyl ring rotors (denoted as PY1 and PY2), as shown in Figure 1c,d. PY1 interacts with a NO_2 (NO_2–π distance: 2.94 Å) or a MeO (CH_3–π distance: 3.37 Å) group, and steric hindrance blocks its rotation. However, PY2 is located side-by-side with PY1. The distances between PY1 and the adjacent PY2 (N–N) are 4.11 and 3.91 Å for CID-5⊃G and CID-6⊃G, respectively, which are slightly smaller than the steric hindrance of ∼4.4 Å (the van der Waals radius and thickness of the pyridyl ring are 2.7 and 1.7 Å, respectively). The crystal structure analyses suggest that the rotational barrier for PY2 should also be high due to the steric hindrance from PY1. However, a molecular dynamics simulation suggested expansion and shrinkage of the distance between PY1 and PY2 with thermal oscillation of the Zn^{2+}–Zn^{2+} bonds in the 2D sheets in both CID-5⊃G and CID-6⊃G (Figure S9). A recent computational study indicated that the oscillation of the local environment around molecular rotors decreases the activation energy for, and thus facilitates, rotation.[13] The oscillation of the 2D sheet is therefore thought to decrease the energy barrier for the rotation of PY2. Indeed, subsequent ^2H solid-state NMR analyses support the rotation of PY2 in CID-5⊃G as described below.

^2H solid-state NMR spectra for CID-5⊃G and CID-6⊃G with deuterated bpy (bpy-d^8) ligands were obtained in order to investigate the rotation of both PY1 and PY2. Simulations of the ^2H solid-state NMR spectra were also calculated in order to elucidate the flip modes and frequencies for the pyridyl rings. It is known that ^2H solid-state NMR analyses are sensitive to molecular rotation in the range 1 kHz to 100 MHz.[14] Figure 2a,b shows the spectra of CID-5⊃G and CID-6⊃G at 298 K, respectively. The spectrum of CID-5⊃G displays three couplets of doublets with splittings of 15.9, 42.5, and 128.9 kHz, which are assigned to a fast 2-site flip, a fast 4-site flip, and a static state on the ^2H NMR scale ($k \leq 1$ kHz), respectively. Considering the steric hindrance of PY1 due to the adjacent 5-NO_2-ip group, this spectral data suggests that PY1 adopts a static mode, while PY2 undergoes both 2-site and 4-site flip rotations (Figure 2c). The disordering of PY2 with a dihedral angle of 24.9° supports the 2-site and 4-site flip rotations. In contrast, the spectrum of CID6⊃G shows a Pake-doublet pattern with a splitting of 128.9 kHz, suggesting that both PY1 and PY2 exist in static states (Figure 2d).

The distance between PY1 and PY2 in CID-5⊃G (N–N: 4.11 Å) is longer than that in CID-6⊃G (N–N: 3.91 Å). The cell volume of CID-5⊃G (989.05 $Å^3$) is also larger than that of CID-6⊃G (958.58 $Å^3$). Such a comparison of the cell volumes in the isostructures reflects the differences in the void spaces of the PCPs. The results also indicate a lower rotational barrier for PY2 in CID-5⊃G, resulting in rotation of PY2 only in CID-5⊃G. Therefore, the differences in the cell volumes for the isostructures induce the large change in the dynamics of PY2. It should therefore be possible to control the rotational frequency of PY2 by employing a solid-solution approach with precise changes in the cell volume according to Vegard's law.

To demonstrate control of the rotational frequency, a series of CID-5/6⊃G (x), $[\{Zn(5\text{-}NO_2\text{-ip})_x(5\text{-}MeO\text{-ip})_{1-x}(bpy\text{-}d^8)\}(DMF{\cdot}MeOH)]_n$, were fabricated, and solid-state ^2H NMR experiments and simulations were performed. X-ray diffraction (XRD) patterns for the CID-5/6⊃G (x) were also obtained. The peak positions in the patterns gradually shift with x, indicating homogeneous distribution of two types of ligands and successful preparation of the solid-solutions (Figure S1). The splitting frequencies and line shapes of the simulated NMR spectra agree well with those of the experimental spectra (Figure S10). Notably, the intensities of the two patterns assigned to the 2-site and 4-site PY2 flip motions gradually increase as the solid-solution ratio x increased from $0 \leq x \leq 0.55$. The calculated flip frequencies for the 4-site flip (Figure 3a) also increase from 1 kHz (x = 0) to 400 kHz (x = 0.55). The increase in the cell

DOI: 10.1021/jacs.5b05413
J. Am. Chem. Soc. 2015, 137, 12183–12186

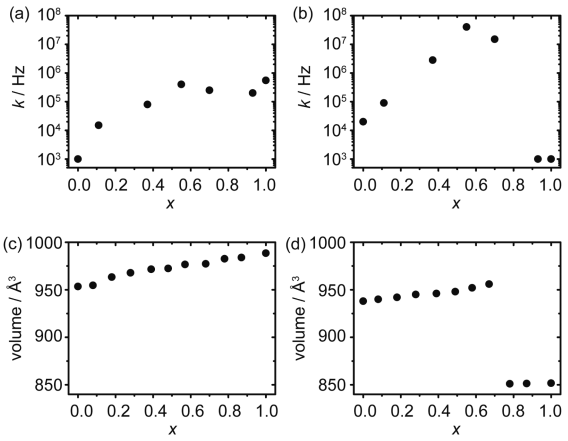

Figure 3. Flip frequencies for 4-site flip rotation as a function of the solid-solution ratio x for (a) CID-5/6⊃G (x) and (b) CID-5/6 (x) at 298 K. Cell volumes for (c) CID-5/6⊃G (x) and (d) CID-5/6 (x). Cell volumes were calculated based on the refinement results for synchrotron powder X-ray diffraction analyses of CID-5/6⊃G (x) and CID-5/6 (x) in which the bpy ligands were not deuterated.[11c]

volume continuously decreases the barriers for PY2 rotation (Figure 3a,c). These results suggest that control of the frequency is feasible by changing the solid-solution ratio. However, the PY2 flip frequency is nearly the same for $0.55 \leq x \leq 1$. A plausible explanation for this behavior is provided below.

After removal of the guest molecules (CID-5/6 (x)), the CID-5/6 (x) exhibited unique properties. Unlike CID-5/6⊃G (x), which had an open-pore form, CID-5/6 (x) had a closed-pore form ($0.78 \leq x \leq 1.0$), indicating that a structural change occurred with an increase in the solid-solution ratio x.[11c] To elucidate the rotation of PY2 after occurrence of this structural change, the solid-state ^{2}H NMR spectra for CID-5/6 (x) were also obtained. Similar to CID-5/6⊃G (x), the flip frequency of the 4-site flip linearly increases for $0 \leq x \leq 0.55$ along with an increase in the cell volume (Figure 3b,d). However, the rotation of PY2 is quenched for $0.93 \leq x \leq 1.0$. This result is attributed to the large change in the crystal structure from the open-pore form to the closed-pore form, which leaves no space for rotation. This structural change derived from the solid solution approach allows to give a wide range of frequency of rotor from 1 kHz to 40 MHz with controllable manner (Figure 4). Interestingly, the maximum frequency (3.2 MHz at $x = 0.55$) for CID-5/6 (x) is higher than

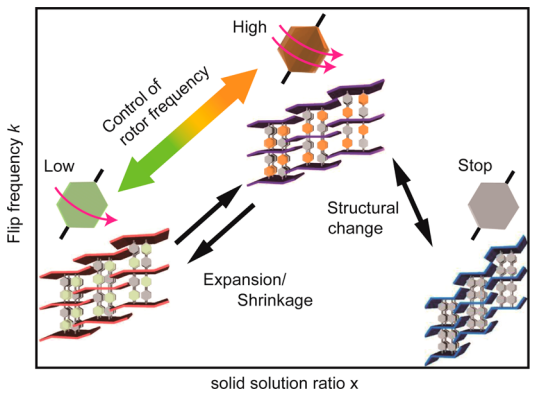

Figure 4. Control of the rotational frequency k of the rotors in solid-solutions of CID-5/6 through modulation of the cell volume by changing the solid-solution ratio x.

that for CID-5/6⊃G (x), suggesting that the guest molecules in CID-5/6⊃G (x) influence the steric hindrance for PY2 rotation and limit the flip frequency for $0.55 \leq x \leq 1$. A recent study on dynamics of molecular rotors also showed that guest molecules in pores affect the rotation of the rotors.[15]

The structural motif for CID-5/6 (x) also consists of π–π stacked 2D sheets, resulting in flexible frameworks. To understand the impact of the flexibility on control of the rotational frequency, solid-solutions of MOFs with robust and cubic-type frameworks were also investigated. Thus, MOF-5 ($[Zn(BDC\text{-}d^4)_x((CH_3)_2\text{-}BDC)_{1-x}]_n$; BDC-$d^4$ = deuterated 1,4-benzenedicarboxylate; $(CH_3)_2$-BDC = 2,5-dimethyl-1,4-benzenedicarboxylate) with x = 0, 0.46, and 1.0 was synthesized.[11b] The phenylene ring rotor of BDC-d^4 was deuterated in order to monitor the rotational frequency using solid-state ^{2}H NMR spectroscopy. XRD patterns of MOF-5 (x) were also obtained. The peak positions are slightly shifted with x, indicating the successful preparation of solid-solutions and little change in the cell volume (Figure S5). Solid-state ^{2}H NMR analyses at 373 K and simulations for MOF-5 (1.0) and MOF-5 (0.46) were then performed (Figure S14). Based on the simulated spectra, it is concluded that the rotors in both MOF-5 (1.0) and MOF-5 (0.46) rotate via a 2-site flip between 0 and 180° at 500 kHz. The rotational behavior of the rotor in MOF-5 (1.0) is similar to that reported previously.[8a] For these MOF-5 solid-solutions, there is no clear difference in the rotational modes and frequencies due to the minimal change in the steric hindrance around the rotor.

Modulation of the cell volume in the solid-solutions of CID-5/6 with flexible frameworks provides control of the rotational frequency of the ligand rotors. However, little change in the cell volume and rotational frequency are observed for solid-solutions of MOF-5 with robust frameworks. An essential factor for control, therefore, is the ability to affect the cell volume and steric hindrance with changes in the solid-solution ratio. In this sense, selected flexible PCPs with interdigitated and interpenetrated frameworks[16] may be suitable platforms for the control of molecular rotors.

In conclusion, we have demonstrated control of the rotational frequency of pillar ligand rotors in PCPs. Changing the solid-solution ratio in solid-solutions of the flexible PCPs effectively modulates the cell volume. This modulation of the cell volume in isostructures reflects variation of the void spaces and results in continuous changes in the barrier for rotation of the rotors, leading to control of the rotational frequency. This study provides the first example of continuous changes in the rotational frequency of molecular rotors in crystalline solids without thermal modulation. It is expected that combination of this method with thermal modulation will offer a wider range of capabilities for the tuning of molecular rotor dynamics with more precision. Furthermore, this strategy should be applicable for the control of the functional dynamics of molecular rotors in other flexible porous materials. There are several examples of MOFs that show continuous change of cell volume by preparation of ligand/metal solid solution,[17] and we believe this family of MOFs could offer more variety of ligand dynamics in a controllable manner. The fine-tuning of ligand dynamics such as rotation and libration in the crystalline framework is related to the functions of dielectricity[18] and ion conductivity,[19] and the control of dynamics of these functional groups aligned in crystals is the next challenge.

DOI: 10.1021/jacs.5b05413
J. Am. Chem. Soc. 2015, 137, 12183–12186

■ ASSOCIATED CONTENT

Supporting Information

The Supporting Information is available free of charge on the ACS Publications website at DOI: 10.1021/jacs.5b05413.

XRD patterns, molecular dynamics simulation, and ^{2}H solid-state NMR spectra (PDF)
(CIF)
(CIF)

■ AUTHOR INFORMATION

Corresponding Authors

*horike@sbchem.kyoto-u.ac.jp
*kitagawa@icems.kyoto-u.ac.jp

Notes

The authors declare no competing financial interest.

■ ACKNOWLEDGMENTS

This work was supported by the PRESTO Program of the Japan Science and Technology Agency (JST) and a Grant-in-Aid for Scientific Research on the Innovative Areas: "Fusion Materials" from the Ministry of Education, Culture, Sports, Science and Technology (MEXT), Japan. iCeMS is supported by the World Premier International Research Initiative (WPI), MEXT, Japan. We are grateful to Prof. M. Mizuno (Kanazawa University) for the program of ^{2}H solid-state NMR simulation.

■ REFERENCES

(1) (a) Balzani, V.; Credi, A.; Raymo, F. M.; Stoddart, J. F. *Angew. Chem., Int. Ed.* **2000**, *39*, 3348−3391. (b) Kottas, G. S.; Clarke, L. I.; Horinek, D.; Michl, J. *Chem. Rev.* **2005**, *105*, 1281−1376. (c) Kay, E. R.; Leigh, D. A.; Zerbetto, F. *Angew. Chem., Int. Ed.* **2007**, *46*, 72−191.

(2) (a) Akutagawa, T.; Nakamura, T. *Dalton Trans.* **2008**, 6335−6345. (b) Comotti, A.; Bracco, S.; Valsesia, P.; Beretta, M.; Sozzani, P. *Angew. Chem., Int. Ed.* **2010**, *49*, 1760−1764. (c) Vogelsberg, C. S.; Garcia-Garibay, M. A. *Chem. Soc. Rev.* **2012**, *41*, 1892−1910.

(3) (a) Horansky, R. D.; Clarke, L. I.; Price, J. C.; Khuong, T.-A. V.; Jarowski, P. D.; Garcia-Garibay, M. A. *Phys. Rev. B: Condens. Matter Mater. Phys.* **2005**, *72*, 014302. (b) Zhang, Q.-C.; Wu, F.-T.; Hao, H.-M.; Xu, H.; Zhao, H.-X.; Long, L.-S.; Huang, R.-B.; Zheng, L.-S. *Angew. Chem., Int. Ed.* **2013**, *52*, 12602−12605. (c) Bracco, S.; Beretta, M.; Cattaneo, A.; Comotti, A.; Falqui, A.; Zhao, K.; Rogers, C.; Sozzani, P. *Angew. Chem., Int. Ed.* **2015**, *54*, 4773−4777.

(4) Akutagawa, T.; Shitagami, K.; Nishihara, S.; Takeda, S.; Hasegawa, T.; Nakamura, T.; Hosokoshi, Y.; Inoue, K.; Ikeuchi, S.; Miyazaki, Y.; Saito, K. *J. Am. Chem. Soc.* **2005**, *127*, 4397−4402.

(5) (a) Setaka, W.; Yamaguchi, K. *Proc. Natl. Acad. Sci. U. S. A.* **2012**, *109*, 9271−9275. (b) Lemouchi, C.; Iliopoulos, K.; Zorina, L.; Simonov, S.; Wzietek, P.; Cauchy, T.; Rodríguez-Fortea, A.; Canadell, E.; Kaleta, J.; Michl, J.; Gindre, D.; Chrysos, M.; Batail, P. *J. Am. Chem. Soc.* **2013**, *135*, 9366−9376.

(6) (a) Garcia-Garibay, M. A. *Proc. Natl. Acad. Sci. U. S. A.* **2005**, *102*, 10771−10776. (b) Khuong, T.-A. V.; Nuñez, J. E.; Godinez, C. E.; Garcia-Garibay, M. A. *Acc. Chem. Res.* **2006**, *39*, 413−422.

(7) (a) Yaghi, O. M.; O'Keeffe, M.; Ockwig, N. W.; Chae, H. K.; Eddaoudi, M.; Kim, J. *Nature* **2003**, *423*, 705−714. (b) Kitagawa, S.; Kitaura, R.; Noro, S. *Angew. Chem., Int. Ed.* **2004**, *43*, 2334−2375.

(8) (a) Gould, S. L.; Tranchemontagne, D.; Yaghi, O. M.; Garcia-Garibay, M. A. *J. Am. Chem. Soc.* **2008**, *130*, 3246−3247. (b) Murdock, C. R.; McNutt, N. W.; Keffer, D. J.; Jenkins, D. M. *J. Am. Chem. Soc.* **2014**, *136*, 671−678.

(9) (a) Horike, S.; Matsuda, R.; Tanaka, D.; Matsubara, S.; Mizuno, M.; Endo, K.; Kitagawa, S. *Angew. Chem., Int. Ed.* **2006**, *45*, 7226−30. (b) Rodríguez-Velamazán, J. A.; González, M. A.; Real, J. A.; Castro, M.; Muñoz, M. C.; Gaspar, A. B.; Ohtani, R.; Ohba, M.; Yoneda, K.; Hijikata, Y.; Yanai, N.; Mizuno, M.; Ando, H.; Kitagawa, S. *J. Am. Chem. Soc.* **2012**, *134*, 5083−5089. (c) Shustova, N. B.; Ong, T.-C.; Cozzolino, A. F.; Michaelis, V. K.; Griffin, R. G.; Dincă, M. *J. Am. Chem. Soc.* **2012**, *134*, 15061−15070.

(10) Vegard, L. *Eur. Phys. J. A* **1921**, *5*, 17−26.

(11) (a) Kleist, W.; Jutz, F.; Maciejewski, M.; Baiker, A. *Eur. J. Inorg. Chem.* **2009**, *2009*, 3552−3561. (b) Deng, H.; Doonan, C. J.; Furukawa, H.; Ferreira, R. B.; Towne, J.; Knobler, C. B.; Wang, B.; Yaghi, O. M. *Science* **2010**, *327*, 846−850. (c) Fukushima, T.; Horike, S.; Inubushi, Y.; Nakagawa, K.; Kubota, Y.; Takata, M.; Kitagawa, S. *Angew. Chem., Int. Ed.* **2010**, *49*, 4820−4824.

(12) Hijikata, Y.; Horike, S.; Tanaka, D.; Groll, J.; Mizuno, M.; Kim, J.; Takata, M.; Kitagawa, S. *Chem. Commun.* **2011**, *47*, 7632−7634.

(13) Jarowski, P. D.; Houk, K. N.; Garcia-Garibay, M. A. *J. Am. Chem. Soc.* **2007**, *129*, 3110−3117.

(14) Rice, D. M.; Wittebort, R. J.; Griffin, R. G.; Meirovitch, E.; Stimson, E. R.; Meinwald, Y. C.; Freed, J. H.; Scheraga, H. A. *J. Am. Chem. Soc.* **1981**, *103*, 7707−7710.

(15) Comotti, A.; Bracco, S.; Ben, T.; Qiu, S.; Sozzani, P. *Angew. Chem., Int. Ed.* **2014**, *53*, 1043−1047.

(16) Schneemann, A.; Bon, V.; Schwedler, I.; Senkovska, I.; Kaskel, S.; Fischer, R. A. *Chem. Soc. Rev.* **2014**, *43*, 6062−6096.

(17) (a) Vujovic, D.; Raubenheimer, H. G.; Nassimbeni, L. R. *Eur. J. Inorg. Chem.* **2004**, *2004*, 2943−2949. (b) Kleist, W.; Maciejewski, M.; Baiker, A. *Thermochim. Acta* **2010**, *499*, 71−78. (c) Burrows, A. D. *CrystEngComm* **2011**, *13*, 3623−3642. (d) Yin, Z.; Zhou, Y. L.; Zeng, M. H.; Kurmoo, M. *Dalton Trans.* **2015**, *44*, 5258−5275.

(18) Chen, S.; Shang, R.; Wang, B. W.; Wang, Z. M.; Gao, S. *Angew. Chem., Int. Ed.* **2015**, *54*, 11093.

(19) Umeyama, D.; Horike, S.; Inukai, M.; Itakura, T.; Kitagawa, S. *J. Am. Chem. Soc.* **2012**, *134*, 12780−12785.

DOI: 10.1021/jacs.5b05413
J. Am. Chem. Soc. 2015, 137, 12183−12186